Article

SOURCE DATA | TRANSPARENT PROCESS | OPEN ACCESS

EMBO reports

E3 ubiquitin ligase NEDD4L negatively regulates inflammation by promoting ubiquitination of MEKK2

Hui Li[1,2,3,†], Ning Wang[1,†], Yu Jiang[1], Haofei Wang[1], Zengfeng Xin[1], Huazhang An[4], Hao Pan[5], Wangqian Ma[6], Ting Zhang[7,*], Xiaojian Wang[1,**] & Wenlong Lin[1,***]

Abstract

Aberrant activation of inflammation signaling triggered by tumor necrosis factor α (TNF-α), interleukin-1 (IL-1), and interleukin-17 (IL-17) is associated with immunopathology. Here, we identify neural precursor cells expressed developmentally down-regulated gene 4-like (NEDD4L), a HECT type E3 ligase, as a common negative regulator of signaling induced by TNF-α, IL-1, and IL-17. NEDD4L modulates the degradation of mitogen-activated protein kinase kinase kinase 2 (MEKK2) via constitutively and directly binding to MEKK2 and promotes its poly-ubiquitination. In interleukin-17 receptor (IL-17R) signaling, *Nedd4l* knockdown or deficiency enhances IL-17-induced p38 and NF-κB activation and the production of proinflammatory cytokines and chemokines in a MEKK2-dependent manner. We further show that IL-17-induced MEKK2 Ser520 phosphorylation is required not only for downstream p38 and NF-κB activation but also for NEDD4L-mediated MEKK2 degradation and the subsequent shutdown of IL-17R signaling. Importantly, *Nedd4l*-deficient mice show increased susceptibility to IL-17-induced inflammation and aggravated symptoms of experimental autoimmune encephalomyelitis (EAE) in IL-17R signaling-dependent manner. These data suggest that NEDD4L acts as an inhibitor of IL-17R signaling, which ameliorates the pathogenesis of IL-17-mediated autoimmune diseases.

Keywords IL-17R signaling; inflammation; MEKK2; NEDD4L; ubiquitination
Subject Categories Immunology; Molecular Biology of Disease; Post-translational Modifications & Proteolysis
DOI 10.15252/embr.202254603 | Revised 25 July 2022 | Accepted 19 August 2022 | Published online 26 September 2022
EMBO Reports (2022) 23: e54603

Introduction

Inflammation represents an adaptive and dynamic host response against pathogens, physical/chemical injuries, toxins, or allergens. The stimulant triggers leukocyte infiltration, cytokines, and chemokines expression, and eventual subsiding of proinflammatory signaling. Dysregulated or prolonged inflammation has been closely related to a variety of human diseases such as autoimmune diseases, cancer, cardiovascular disease, and metabolic disorders (Coussens & Werb, 2002; Hotamisligil, 2017; Liu *et al*, 2020). Thus, immune-regulatory and negative feedback mechanisms are critically required to harness inflammation and prevent excessive immunopathology post-inflammation (Medzhitov, 2008).

Inflammatory cytokines such as tumor necrosis factor α (TNF-α), interleukin-1 (IL-1), and interleukin-17 (IL-17) are key regulators in the inflammation process. By binding IL-1R, IL-1 activates the MyD88-IRAK1-TRAF6-TAK1 cascade (Boraschi *et al*, 2018). TNF-α exerts its biological effects by binding two different receptors, TNFR1 and TNFR2. Upon activation, TNFR1 recruits adaptor proteins including TRADD, TRAF2, cIAP1, cIAP2, and RIP1. TNFR2 recruits TRAF2 and also TRAF1, TRAF3, cIAP1, and cIAP2, through their binding to TRAF2 (Kalliolias & Ivashkiv, 2016). Although with different biological functions, both IL-1 and TNF-α activate downstream MAPK and NF-κB to induce inflammatory responses. Among the six members of the IL-17 family (i.e., IL-17A to IL-17F), IL-17A, commonly called IL-17, is the first identified and also the most intensively studied member (Iwakura *et al*, 2011). IL-17F shares the strongest sequence homology with IL-17A. IL-17A and IL-17F activate downstream signaling pathways through a heterodimeric receptor composed of the IL-17RA and IL-17RC subunits (Gaffen, 2009). Upon IL-17 and IL-17F ligation, IL-17RA and IL-17RC recruit TRAF6

1 Institute of Immunology and Department of Orthopedic Surgery, The Second Affiliated Hospital, Zhejiang University School of Medicine, Zhejiang, China
2 Department of Medical Oncology, The Cancer Hospital of the University of Chinese Academy of Sciences (Zhejiang Cancer Hospital), Hangzhou, China
3 Institute of Basic Medicine and Cancer (IBMC), Chinese Academy of Sciences, Hangzhou, China
4 Shandong Provincial Key Laboratory for Rheumatic Disease and Translational Medicine, The First Affiliated Hospital of Shandong First Medical University & Shandong Provincial Qianfoshan Hospital, Jinan, China
5 Department of Urology, The First Affiliated Hospital, College of Medicine, Zhejiang University, Hangzhou, China
6 Department of Gastroenterology, The Second Affiliated Hospital, Zhejiang University School of Medicine, Hangzhou, China
7 Department of Radiation Oncology, The Second Affiliated Hospital, Zhejiang University School of Medicine, Hangzhou, China
*Corresponding author. Tel: +86 0571 87783538; E-mail: zezht@zju.edu.cn
**Corresponding author. Tel: +86 0571 88206160; E-mail: wangxiaojian@cad.zju.edu.cn
***Corresponding author. Tel: +86 571 88981662; E-mail: lwl210@foxmail.com
†These authors contributed equally to this work

through adaptor protein Act1, ultimately activating MAPK, NF-κB, C/EBPδ, and C/EBPβ to induce proinflammatory cytokines and chemokines expression (Qu *et al*, 2012).

TNF-α-, IL-1-, and IL-17-induced signaling pathway protectively responds to pathogen invasion, injuries, toxins, and allergens. However, prolonged activated TNF-α-, IL-1-, and IL-17-induced signaling will cause the development of autoimmune diseases such as experimental autoimmune encephalomyelitis (EAE) (Sutton *et al*, 2009; Rostami & Ciric, 2013; Wolf *et al*, 2017). As is well demonstrated, deficiency or destruction of the negative regulator of the inflammatory signaling is responsible for the development of autoimmune diseases. As a negative regulator involved in TNF-α- and IL-1-induced inflammatory signaling pathway, TNF-α-induced protein 3 (TNFIP3, also known as A20) has been reported to be associated with many human inflammation-related diseases (Catrysse *et al*, 2014).

Neural precursor cell expressed developmentally down-regulated gene 4-like (NEDD4L) is a highly conserved HECT-type E3 ligase. NEDD4L mediates ubiquitination of epithelial Na^+ channel (ENaC) and inhibits cell surface expression of ENaC in epithelia (Goulet *et al*, 1998; Abriel *et al*, 1999). NEDD4L also limits TGF-β signal transduction by mediating Smad2/3 poly-ubiquitination and degradation (Gao *et al*, 2009). NEDD4L has been reported to be associated with nerve disease in human and mouse models (Charbonnier-Beaupel *et al*, 2015; Jewett *et al*, 2016; Manning & Kumar, 2018). Our recent data demonstrate that NEDD4L promotes Lys-29-linked ubiquitination of TRAF3, and thus positively regulates antivirus innate response (Gao *et al*, 2021). We also showed in a previous study that NEDD4L negatively regulates keratinocyte hyperplasia by promoting Lys-27-linked ubiquitination of GP130 and proteasomal degradation in keratinocytes (Liu *et al*, 2021). However, the physiologic role of NEDD4L in autoimmune diseases remains largely unknown.

In the present study, we identify NEDD4L as a common negative regulator of IL-17-, TNF-α-, and IL-1α-induced signaling. NEDD4L constitutively and directly binds MEKK2 and reduces MEKK2 expression by promoting K27-linked poly-ubiquitination of MEKK2. *Mekk2* knockdown inhibits IL-17-induced p38 and NF-κB activation, as well as IL-17-induced proinflammatory cytokine and chemokine production. NEDD4L inhibits IL-17-induced inflammation in a MEKK2-dependent manner. Further study shows that IL-17 induces MEKK2 Ser520 phosphorylation, which is not only crucial for the activation of p38 and NF-κB pathways but also for NEDD4L-mediated MEKK2 degradation to suppress IL-17R signaling. Furthermore, *Nedd4l*-deficient mice are more susceptible to IL-17-induced peritonitis and pneumonia, and IL-17R-related EAE. These results suggest that as a negative regulator of MEKK2-dependent IL-17R-mediated inflammation, NEDD4L severs as a pivotal immune modulator for dysregulated inflammation-mediated autoimmune diseases.

Results

NEDD4L negatively regulates IL-17-, TNF-α-, and IL-1α-induced inflammation

To explore the role of NEDD4L in inflammation, we determined the effect of *Nedd4l* knockdown on IL-17-induced proinflammatory cytokine and chemokine expression. Synthesized *Nedd4l*-specific small-interfering RNA (si*Nedd4l*) was transfected into HeLa cells to inhibit endogenous NEDD4L expression (Fig EV1A). *Nedd4l* knockdown significantly increased IL-17-induced *Il-6*, *Cxcl2*, *Ccl20* mRNA expression, and IL-6 and CXCL2 production (Fig 1A and B). We next investigated the role of NEDD4L in inflammatory responses in embryonic fibroblasts (MEFs), which is well established for the IL-17R signaling study (Zhong *et al*, 2012). As shown in Fig 1C and D, IL-17-induced *Il-6*, *Cxcl2*, and *Ccl20* mRNA expression, and IL-6 and CXCL2 production were significantly increased in MEFs with *Nedd4l* homozygous deficiency ($Nedd4l^{-/-}$) compared to the wild-type ($Nedd4l^{+/+}$) MEFs. Since IL-17F has similar functions as IL-17, *Nedd4l* homozygous deficiency significantly increased IL-17F-induced *Il-6*, *Cxcl2*, and *Ccl20* mRNA expression in MEFs (Fig 1E). Such significantly increased IL-17A- or IL-17F-induced *Il-6*, *Cxcl2*, and *Ccl20* mRNA expression were also observed in MEFs with *Nedd4l* heterozygous deficiency ($Nedd4l^{+/-}$) (Fig EV1B–D). Lung epithelial cells and astrocytes have been also identified to play a crucial role in IL-17-induced inflammation and autoimmune diseases (Kang *et al*, 2010; Zhong *et al*, 2012). *Nedd4l* deficiency in these cells resulted in significantly increased IL-17-induced *Il-6*, *Cxcl2*, and *Ccl20* mRNA expression compared to the wild-type control cells (Figs 1F and G, and EV1E and F). These results suggest that NEDD4L plays a crucial role in IL-17-induced inflammation *in vitro*.

Interestingly, increased TNF-α- or IL-1α-induced *Il-6*, *Cxcl2*, and *Ccl20* mRNA expression was also observed in HeLa cells with *Nedd4l* knockdown and in MEFs with *Nedd4l* deficiency (Fig EV2A–D). These data suggest that NEDD4L might be a common negative regulator of TNF-α-, IL-1α-, and IL-17-induced inflammation.

NEDD4L inhibits IL-17-induced inflammation *in vivo*

To explore the regulatory role of NEDD4L in IL-17-induced inflammation responses *in vivo*, $Nedd4l^{+/+}$ and $Nedd4l^{+/-}$ mice were

Figure 1. NEDD4L negatively regulates IL-17-induced proinflammatory cytokine expression.

A, B HeLa cells were transfected with *Nedd4l* siRNA (si*Nedd4l*) or control RNA (si*NC*). *Il-6*, *Cxcl2*, and *Cccl20* mRNA expression (A) and ELISA assay of IL-6 and CXCL2 production (B) in HeLa cells transfected with *Nedd4l* siRNA (si*Nedd4l*) or control RNA (si*NC*) and stimulated with IL-17 (50 ng/ml) for the indicated time (n = 3 technical replicates).

C, D Real-time PCR analysis of *Il-6*, *Cxcl2*, and *Cccl20* mRNA expression (C) and ELISA assay of IL-6 and CXCL2 production (D) in wild-type ($Nedd4l^{+/+}$) and *Nedd4l*-deficient homozygous ($Nedd4l^{-/-}$) MEFs following stimulation with IL-17 (100 ng/ml) for the indicated time (n = 3 technical replicates).

E Real-time PCR analysis of *Il-6*, *Cxcl2*, and *Ccl20* mRNA expression in $Nedd4l^{+/+}$ and $Nedd4l^{-/-}$ MEFs following stimulation with IL-17F (100 ng/ml) (n = 3 technical replicates).

F, G Real-time PCR analysis of *Il-6*, *Cxcl2*, and *Cccl20* mRNA in $Nedd4l^{+/+}$ and $Nedd4l^{-/-}$ primary lung epithelial cells (F), or in $Nedd4l^{+/+}$ and $Nedd4l^{+/-}$ primary astrocytes (G) untreated or stimulated with IL-17 (100 ng/ml) for the indicated time (n = 3 technical replicates).

Data information: Data are shown as the mean ± S.E.M. of technical replicates. Experiments were performed three times (A-E) or two times (F, G), and representative data are shown. Significant differences were tested using a two-tailed Student's *t*-test. *P < 0.05, **P < 0.01, ***P < 0. 001. NS, no significance.

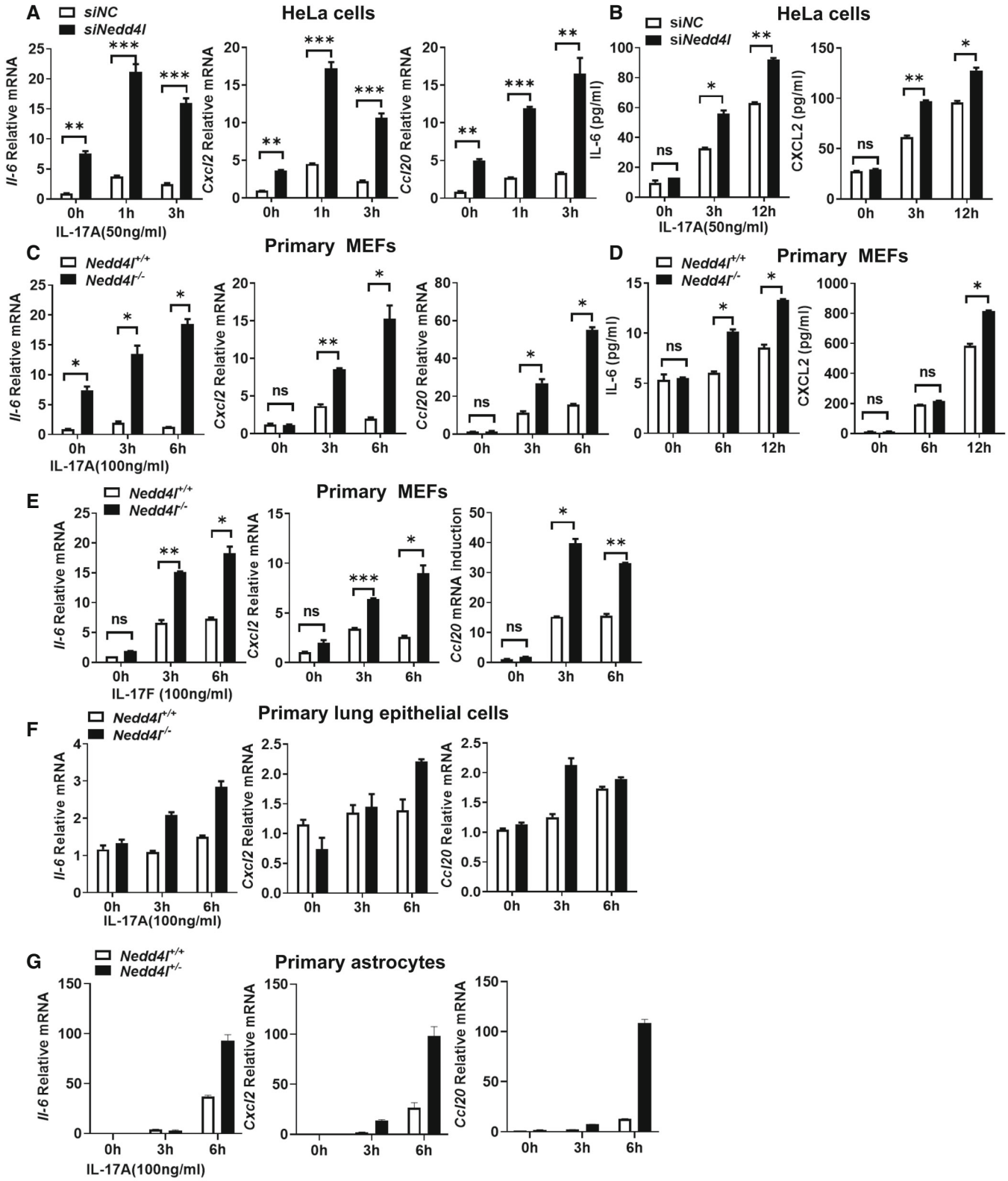

Figure 1.

intraperitoneally injected (*i.p.*) with IL-17 or PBS, and *Il-6*, *Cxcl2*, and *Ccl20* mRNA expression in peritoneal mesothelial cells were analyzed by real-time PCR. As shown in Figs 2A and EV2E, *Nedd4l* deficiency significantly increased IL-17-induced *Il-6*, *Cxcl2*, and *Ccl20* mRNA expression in peritoneal mesothelial cells. IL-17-induced chemokines amplify inflammatory responses by recruiting

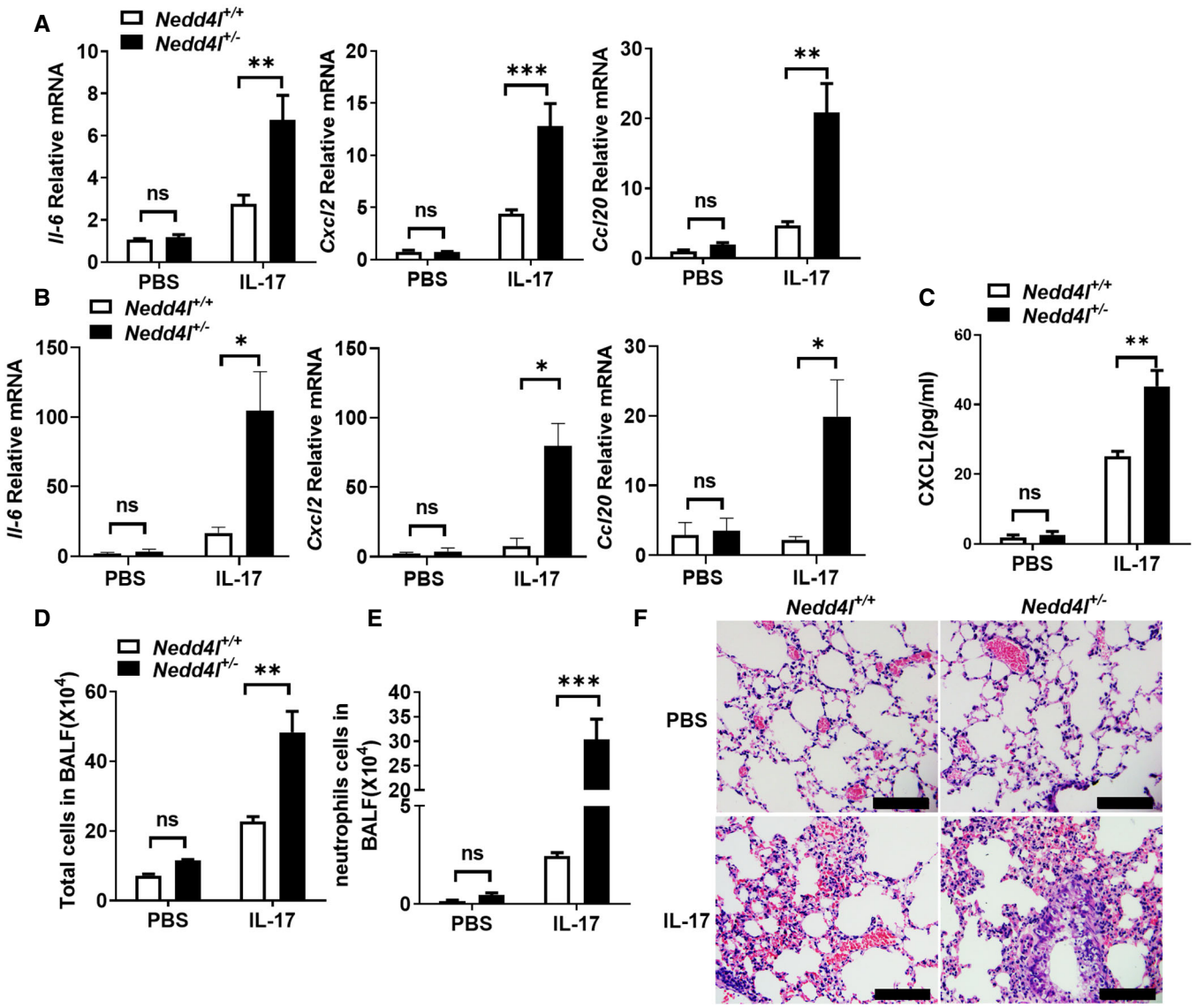

Figure 2. NEDD4L restricts IL-17-induced inflammation.

A Real-time PCR analysis of *Il-6*, *Cxcl2*, and *Cccl20* mRNA expression in peritoneal mesothelial cells isolated from *Nedd4l*$^{+/+}$ and *Nedd4l*$^{+/-}$ mice treated by intraperitoneal injection of PBS (n = 4 biological replicates) or IL-17 (n = 6 biological replicates) (0.5 μg in 200 μl PBS).

B Real-time PCR analysis of *Il-6*, *Cxcl2*, and *Cccl20* mRNA expression in lung tissue of *Nedd4l*$^{+/+}$ and *Nedd4l*$^{+/-}$ mice (n = 3 biological replicates) treated by intratracheal injection of PBS or IL-17 (2 μg in 30 μl PBS).

C ELISA assay of CXCL2 production in BALF from mice treated as in (B) (n = 3 biological replicates).

D, E Infiltration of total CD45$^+$ cells (D) and Gr-1$^+$CD11b$^+$ cells (E) in BALF from mice treated as in (B) (n = 3 biological replicates).

F Hematoxylin and eosin staining of lung tissue from mice treated as in (B). Scale bars, 100 μm.

Data information: Data are shown as the mean ± S.E.M. of biological replicates. All experiments were performed two times, and representative data are shown. Significant differences were tested using a two-tailed Student's t-test. *P < 0.05, **P < 0.01, and ***P < 0. 001. NS, no significance.

neutrophils to local tissue, as shown in an inflammation model in which airway administration of IL-17 caused considerable pulmonary inflammation (Bulek *et al*, 2011; Zhong *et al*, 2012). To determine whether NEDD4L affects IL-17-induced pulmonary inflammation, *Nedd4l*$^{+/+}$ and *Nedd4l*$^{+/-}$ mice were intratracheally injected with IL-17 or PBS, followed by the analysis of *Il-6*, *Cxcl2*, and *Ccl20* mRNA expression in lung tissues and production of CXCL2 in the bronchoalveolar lavage fluid (BALF). As shown in Fig 2B, *Nedd4l* deficiency significantly increased IL-17-induced *Il-6*, *Cxcl2*, and *Ccl20* mRNA expression in lung tissues. CXCL2 production in BALF from *Nedd4l*$^{+/-}$ mice was also significantly increased compared to that from *Nedd4l*$^{+/+}$ mice (Fig 2C). Consistent with increased proinflammatory cytokine and chemokine production in *Nedd4l*$^{+/-}$ mice, more CD45$^+$ cells were recruited into the BALF of

Nedd4l$^{+/-}$ mice than that of *Nedd4l*$^{+/+}$ mice (Fig 2D). In particular, neutrophils (Gr1^{+}CD11b^{+}) in the BALF of *Nedd4l*$^{+/-}$ mice were increased more than 10 folds compared with that in wild-type mice (Fig 2E), indicating that *Nedd4l* deficiency increased IL-17-induced pulmonary neutrophil infiltration. Histological analysis of lung tissue showed enhanced immunopathological changes in the lungs of *Nedd4l*$^{+/-}$ mice (Fig 2F). These results suggest that NEDD4L plays an important role in limiting IL-17-induced inflammation *in vivo*.

NEDD4L inhibits IL-17R signaling and MEKK2 expression

IL-17 induces proinflammatory cytokine and chemokine production through MAPK and NF-κB pathways. In HeLa cells, *Nedd4l* knockdown increased IL-17-induced phosphorylation of p38 and NF-κB p65 subunit without affecting IL-17-induced phosphorylation of ERK1/2 and JNK1/2 (Fig 3A). In MEFs, *Nedd4l* deficiency increased IL-17-induced p38 and NF-κB p65 subunit phosphorylation but not ERK1/2 and JNK1/2 phosphorylation (Fig 3B). Accordingly, *Nedd4l* knockdown in HeLa cells or deficiency in MEFs remarkably increased TNF-α- or IL-1α-induced p38 and NF-κB p65 phosphorylation (Fig EV3A–D). Consistently, *Nedd4l* deficiency in primary lung epithelial cells and astrocytes significantly promoted IL-17-induced p38 and NF-κB p65 subunit phosphorylation (Fig 3C and D). Overexpression of exogenous wild-type NEDD4L, but not the E3 enzyme activity mutation NEDD4L-C942A (NEDD4L-CA) in HeLa cells, inhibited IL-17-induced p38 and NF-κB p65 subunit phosphorylation compared to the control group (Fig 3E). Similar signal transduction effect mediated by overexpression of exogenous NEDD4L could be reconstituted in *Nedd4l*-silenced HeLa cells, suggesting that NEDD4L specifically regulates this signaling (Fig EV3E). These results indicate that NEDD4L plays a negative regulatory role in IL-17-induced signaling.

IL-17RA and IL-17RC activate MAPKs and NF-κB pathways through TRAF family members. However, neither *Nedd4l* knockdown nor *Nedd4l* deficiency affected expressions of the TRAFs (Fig 3A and B). Given the important role of MEKK family members in MAPK and NF-κB activation (Zhao & Lee, 1999; Blonska *et al*, 2004), we set out to investigate the effect of *Nedd4l* knockdown on MEKKs. Interestingly, *Nedd4l* knockdown significantly increased MEKK2 expression in HeLa cells (Fig 3A). In MEFs, primary lung epithelial cells, and astrocytes, *Nedd4l* deficiency also increased MEKK2 expression (Fig 3B–D). Overexpression or reconstitution of exogenous wild-type NEDD4L, but not NEDD4L-CA, can inhibit MEKK2 expression compared to the control group (Figs 3E and EV3E). We compared MEKK2 expression in *Nedd4l*$^{+/-}$, *Nedd4l*$^{-/-}$, and wild-type MEFs. As shown in Fig 3F, *Nedd4l* heterozygous deficiency was sufficient to increase MEKK2 expression in MEFs. Notably, *Nedd4l* deficiency in MEFs strongly prolonged the half-life of MEKK2 protein compared to that in wild-type MEFs (Fig 3G and H). Furthermore, overexpression of NEDD4L reduced MEKK2 expression (Fig EV3F), providing further evidence that NEDD4L inhibits the stability of MEKK2 protein.

NEDD4L mediates MEKK2 ubiquitination

To determine the mechanism through which NEDD4L reduced MEKK2 expression, we investigated the interaction between NEDD4L and MEKK2 in HeLa cells by immunoprecipitation with NEDD4L- or MEKK2-specific antibody. As shown in Figs 4A and EV4A, NEDD4L was co-immunoprecipitated with MEKK2, but not MEKK3, in both IL-17-stimulated and unstimulated cells, suggesting that NEDD4L was constitutively associated with MEKK2 in HeLa cells. In the pull-down assay, NEDD4L recombinant protein was precipitated with GST-MEKK2 protein (Fig 4B), suggesting that NEDD4L bound MEKK2 *in vitro*. To map the domains required for NEDD4L to interact with MEKK2, we constructed a series of plasmids expressing wild-type and mutant NEDD4L in which C2 (ΔC2), WW (ΔWW), or HECT (ΔHECT) domain was deleted, respectively (Fig EV4B). As shown in Fig 4C, the deletion of the WW domain but not the C2 and HECT domain disrupted the interaction between NEDD4L and MEKK2, demonstrating that the WW domain was necessary for NEDD4L to bind to MEKK2. As an E3 ubiquitin ligase, NEDD4L might inhibit the stability of MEKK2 protein by mediating the ubiquitination of MEKK2. To investigate whether NEDD4L regulates MEKK2 expression through proteasome-dependent or lysosomal-dependent pathway, we treated *Nedd4l*$^{-/-}$ and wild-type control MEFs with a proteasome inhibitor MG132 or a lysosomal degradation inhibitor bafilomycin A1 (Baf A1). Following MG132 treatment but not Baf A1 treatment, MEKK2 expression in wild-type control cells was elevated to the level comparable with that in *Nedd4l*$^{-/-}$ MEFs (Fig 4D), suggesting that NEDD4L suppresses the stability of MEKK2 protein by mediating MEKK2 ubiquitination in a proteasome-dependent manner. In further support of our hypothesis, *in vitro* ligase activity assay demonstrated that it was NEDD4L protein, but not TRAF6 protein, efficiently increased MEKK2 ubiquitination (Fig 4E), suggesting that MEKK2 is a potential substrate of NEDD4L. Furthermore, NEDD4L deficiency reduced total polyubiquitination of MEKK2, without affecting K63- and K48-linked

Figure 3. NEDD4L inhibits IL-17R signaling and MEKK2 expression.

A–D Immunoblot analysis of phosphorylated ERK1/2 (P-ERK1/2), phosphorylated p38 (P-P38), phosphorylated JNK1/2 (P-JNK1/2), phosphorylated p65 subunit of NF-κB (P-P65), total P65, MEKK2, TRAF2, TRAF3, TRAF6, NEDD4L, and actin in HeLa cells transfected with *Nedd4l* siRNA (si*Nedd4l*) or control RNA (si*NC*) (A), *Nedd4l*$^{+/+}$ and *Nedd4l*$^{-/-}$ MEFs (B), primary lung epithelial cells (C), or *Nedd4l*$^{+/+}$ and *Nedd4l*$^{+/-}$ astrocytes (D), treated with IL-17 for indicated time.

E Immunoblot analysis of phosphorylated p65 subunit of NF-κB (P-P65), total P65, phosphorylated p38 (P-P38), total P38, MEKK2, NEDD4L, and actin in HeLa cells transfected with Myc-tagged NEDD4L, Myc-tagged NEDD4L-CA(C942A), or Myc-tagged Null plasmids, treated with IL-17 for the indicated time.

F Immunoblot analysis of MEKK2, TRAF2, TRAF6, NEDD4L, and actin in *Nedd4l*$^{+/+}$, *Nedd4l*$^{+/-}$, and *Nedd4l*$^{-/-}$ MEFs.

G Immunoblot analysis of MEKK2 in lysates of *Nedd4l*$^{+/+}$ and *Nedd4l*$^{-/-}$ MEFs treated with CHX (50 μg/ ml) for the indicated time.

H The intensity values were measured by Image J software to calculate the half-life of MEKK protein (n = 3 biological replicates).

Data information: Numbers between two blots indicate the densitometry of phosphorylated proteins relative to that of total proteins, respectively. Densitometry of MEKK2 was relative to actin. All experiments were performed three times, and representative data are shown. Significant differences were tested using a two-tailed Student's t-test. *P < 0.05 and **P < 0.01. NS, no significance.
Source data are available online for this figure.

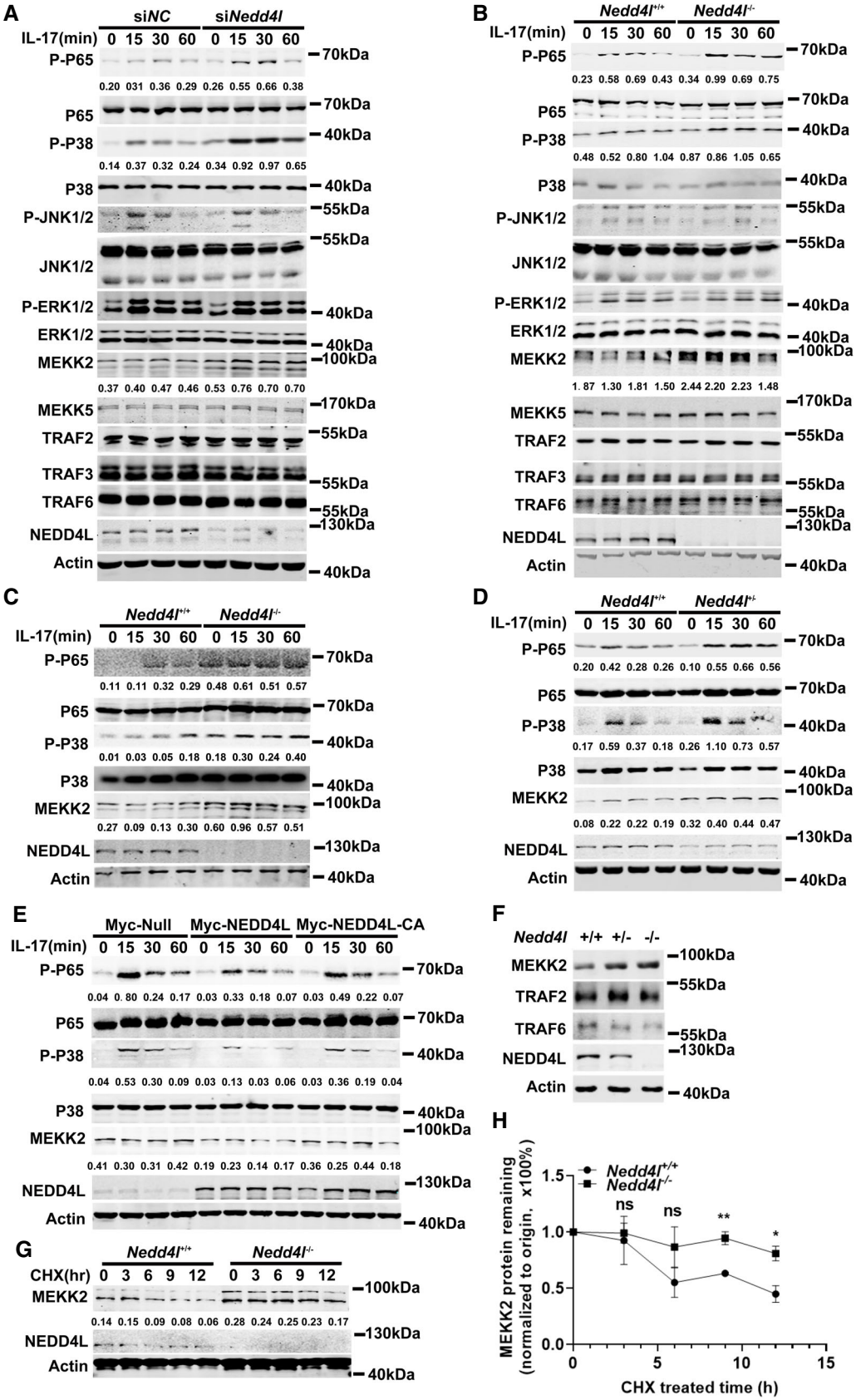

Figure 3.

poly-ubiquitination of MEKK2 in MEFs (Fig 4F). We further determined the effects of wild-type versus mutant NEDD4L on MEKK2 ubiquitination in HEK293T cells. NEDD4L-ΔWW completely lost the capability to promote MEKK2 ubiquitination. Furthermore, deletion of the HECT domain also largely impaired such capability of NEDD4L. In contrast, deletion of the C2 domain enhanced the

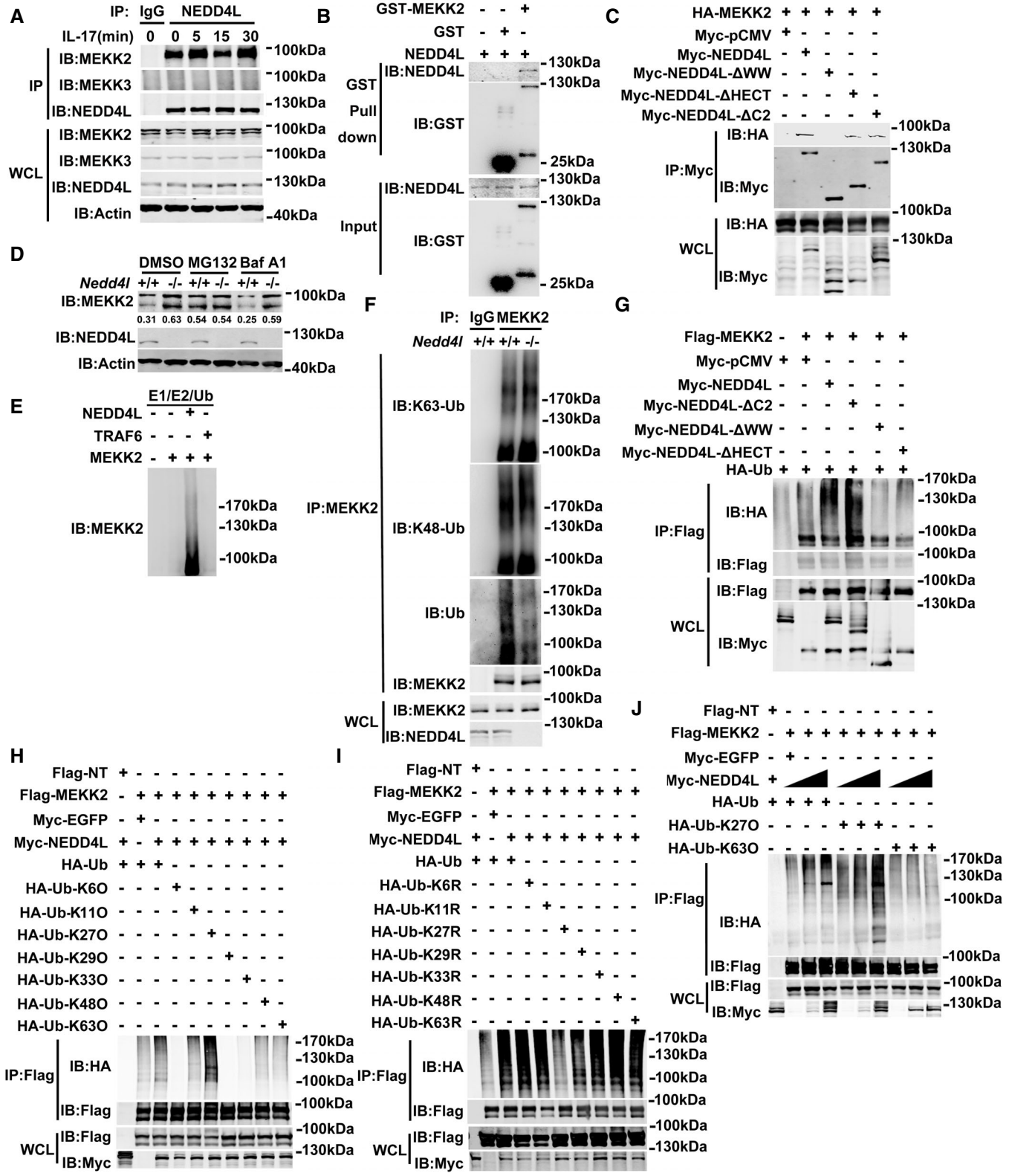

Figure 4.

Figure 4. NEDD4L ubiquitinates MEKK2 and inhibits the protein stability of MEKK2.

A Immunoblot analysis of NEDD4L, MEKK2, and MEKK3 immunoprecipitated with NEDD4L-specific antibody from lysates of HeLa cells pre-treated with 20 μM MG-132 for 6 h and then treated with IL-17 for the indicated time.

B Immunoblot analysis of NEDD4L precipitated with GST-tagged Null or GST-tagged MEKK2 recombinant protein.

C Immunoblot of HA-tagged MEKK2 co-immunoprecipitated with anti-Myc antibody from lysates of HEK293T cells co-transfected with plasmids expressing HA-tagged MEKK2 and Myc-tagged wild-type NEDD4L or mutant NEDD4L with C2 (ΔC2), WW (ΔWW), or HECT (ΔHECT) domain deleted.

D Immunoblot analysis of MEKK2 and NEDD4L in *Nedd4l*$^{+/+}$, and *Nedd4l*$^{-/-}$ treated with DMSO, 20 μM MG-132, or 0.2 μM bafilomycin A1 (Baf A1) for 6 h. Densitometry of MEKK2 was relative to actin.

E Immunoblot analysis of MEKK2 incubated with NEDD4L or TRAF6 recombinant protein and the full complement of ubiquitination reaction components *in vitro*.

F Immunoblot analysis of K48-, K63-linked, and total ubiquitination of MEKK2 following precipitation of MEKK2 with MEKK2-specific antibody from lysates of *Nedd4l*$^{+/+}$ and *Nedd4l*$^{-/-}$ MEFs treated with MG-132.

G Immunoblot analysis of total ubiquitination of Flag-tagged MEKK2 following precipitation of MEKK2 with Flag-tagged specific antibody from lysates of HEK293T cells co-transfected with plasmids expressing Flag-tagged MEKK2 and Myc-tagged wild-type NEDD4L or mutant NEDD4L with C2 (ΔC2), WW (ΔWW), or HECT (ΔHECT) domain deleted.

H Immunoblot analysis of total ubiquitination of Flag-tagged MEKK2 following immunoprecipitating MEKK2 with anti-Flag antibody from lysates of HEK293T cells co-transfected with plasmids expressing Flag-tagged MEKK2, Myc-tagged NEDD4L, and HA-tagged wild-type or K6O, K11O, K27O, K29O, K33O, K48O, and K63O mutant Ub.

I Immunoblot analysis of total ubiquitination of Flag-tagged MEKK2 following immunoprecipitating MEKK2 with anti-Flag antibody from lysates of HEK293T cells co-transfected with plasmids expressing Flag-tagged MEKK2, Myc-tagged NEDD4L, and HA-tagged wild-type or K6R, K11R, K27R, K29R, K33R, K48R, K63R mutant Ub.

J Immunoblot analysis of total ubiquitination of Flag-tagged MEKK2 following immunoprecipitating MEKK2 with anti-Flag antibody from lysates of HEK293T cells co-transfected with plasmids expressing Flag-tagged MEKK2, increased dosage of Myc-tagged NEDD4L, and HA-tagged wild-type, K27O, or K63O mutant Ub.

Data information: All experiments were performed three times, and representative data are shown.
Source data are available online for this figure.

ubiquitination of MEKK2, which could be due to the relief of autoinhibitory interaction between its C2 and HECT domains, consistent with the notion that the C2 domain of HECT family ligases, including smurf2, NEDD4, and NEDD4L, inhibits the function of HECT domain (Wang *et al*, 2010; Malonis *et al*, 2017; Lorenz, 2018; Fig 4G). To determine the nature of NEDD4L-mediated MEKK2 ubiquitination, we transfected HEK293T cells with NEDD4L- and MEKK2-expressing vectors in the presence of constructs expressing wild-type ubiquitin (HA-Ub) or its mutants. As shown in Fig 4H and I, NEDD4L mainly promoted Lys-27(K27O)-linked poly-ubiquitination of MEKK2 (Fig 4H). Mutation of Lys-27 (K27R) completely abrogated the poly-ubiquitination effect of NEDD4L on MEKK2 (Fig 4I), demonstrating that NEDD4L mediates K27-linked poly-ubiquitination of MEKK2. It is well established that the ubiquitin chain specificity of the HECT-type E3 ligases is determined by their C-terminal amino acids. NEDD4 family ligases, including NEDD4L, exhibit strict specificity toward K63 linkages (Maspero *et al*, 2013). However, in our study, NEDD4L mediates K27-linked but not K63-linked poly-ubiquitination of MEKK2 in a dosage-dependent manner (Fig 4J), which could be a consequence of the unique structure of NEDD4L. Further studies will be needed to identify the detailed differences between NEDD4L and other HECT-type E3 ligases.

MEKK2 is required for IL-17R signaling

MEKK2 has been reported to participate in TNF-α- and IL-1-induced signaling (Chayama *et al*, 2001; Hammaker *et al*, 2004). However, it remains unknown whether MEKK2 is also involved in IL-17R signaling. Thus, our further experiments were focused on the role of MEKK2 in NEDD4L-mediated negative regulation of IL-17R signaling. We firstly used synthesized *Mekk2*-specific small-interfering RNA (si*Mekk2*) to inhibit endogenous MEKK2 expression in HeLa cells, and then stimulated the cells with IL-17 and detected IL-17-induced MAPKs and NF-κB activation. As shown in Fig 5A, *Mekk2* siRNA inhibited endogenous MEKK2 expression and IL-17-induced p38 and NF-κB activation. Consistently, *Mekk2* siRNA inhibited IL-17-induced *Il-6*, *Cxcl2*, and *Ccl20* mRNA expression in HeLa cells (Fig 5C). Similarly, *Mekk2* knockdown also inhibited IL-17-induced p38 and NF-κB activation and *Il-6*, *Cxcl2*, and *Ccl20* mRNA expression in MEFs (Fig 5B–D). These results suggest that MEKK2 is required for IL-17R signaling.

To investigate the role of MEKK2 in NEDD4L-mediated regulation of IL-17R signaling, we compared the effects of *Nedd4l* siRNA on IL-17-induced p38 and NF-κB activation in the presence and absence of *Mekk2* siRNA. As shown in Fig 5E, transfection of *Nedd4l* siRNA alone enhanced IL-17-induced p38 and NF-κB activation in HeLa

Figure 5. NEDD4L inhibits IL-17R signaling by targeting MEKK2.

A, B Immunoblot analysis of phosphorylated p38 (P-P38), phosphorylated NF-κB p65 (P-P65), MEKK2, and actin in HeLa cells (A), and MEFs (B) transfected with *Mekk2* siRNA (si*Mekk2*) or control RNA (si*NC*) and stimulated with IL-17 (HeLa cells 50 ng/ml, MEFs 100 ng/ml) for the indicated time.

C, D Real-time PCR analysis of *Il-6*, *Cxcl2*, and *Ccl20* mRNA expression in HeLa cells (C) and MEFs (D) transfected with siRNA (si*Mekk2*) or control RNA (si*NC*) and stimulated with IL-17 (HeLa cells 50 ng/ml, MEFs 100 ng/ml) for the indicated time (n = 3 technical replicates).

E Immunoblot analysis of phosphorylated p38, phosphorylated NF-κB p65 (P-P65), NEDD4L, MEKK2, and actin in HeLa cells transfected with control RNA (si*NC*), *Nedd4l* siRNA (si*Nedd4l*), *Mekk2* siRNA(si*Mekk2*), or *Nedd4l* siRNA plus *Mekk2* siRNA (si*Nedd4l* + si*Mekk2*), and stimulated with IL-17 (50 ng/ml) for the indicated time.

F Immunoblot analysis of phosphorylated p38, phosphorylated NF-κB p65 (p-p65), NEDD4L, MEKK2, and actin in *Nedd4l*$^{+/+}$ and *Nedd4l*$^{-/-}$ MEFs transfected with *Mekk2* siRNA (si*Mekk2*) or control RNA (si*Nc*), and stimulated with IL-17 (100 ng/ml) for the indicated time.

G, H Real-time PCR analysis of *Il-6*, *Cxcl2*, and *Ccl20* mRNA expression in HeLa cells (G) and MEFs (H) treated as described in (E) and (F) (n = 3 technical replicates).

Data information: Numbers between two blots indicate the densitometry of phosphorylated proteins relative to that of total proteins, respectively. Data are shown as the mean ± S.E.M. of technical replicates. All experiments were performed two times, and representative data are shown.
Source data are available online for this figure.

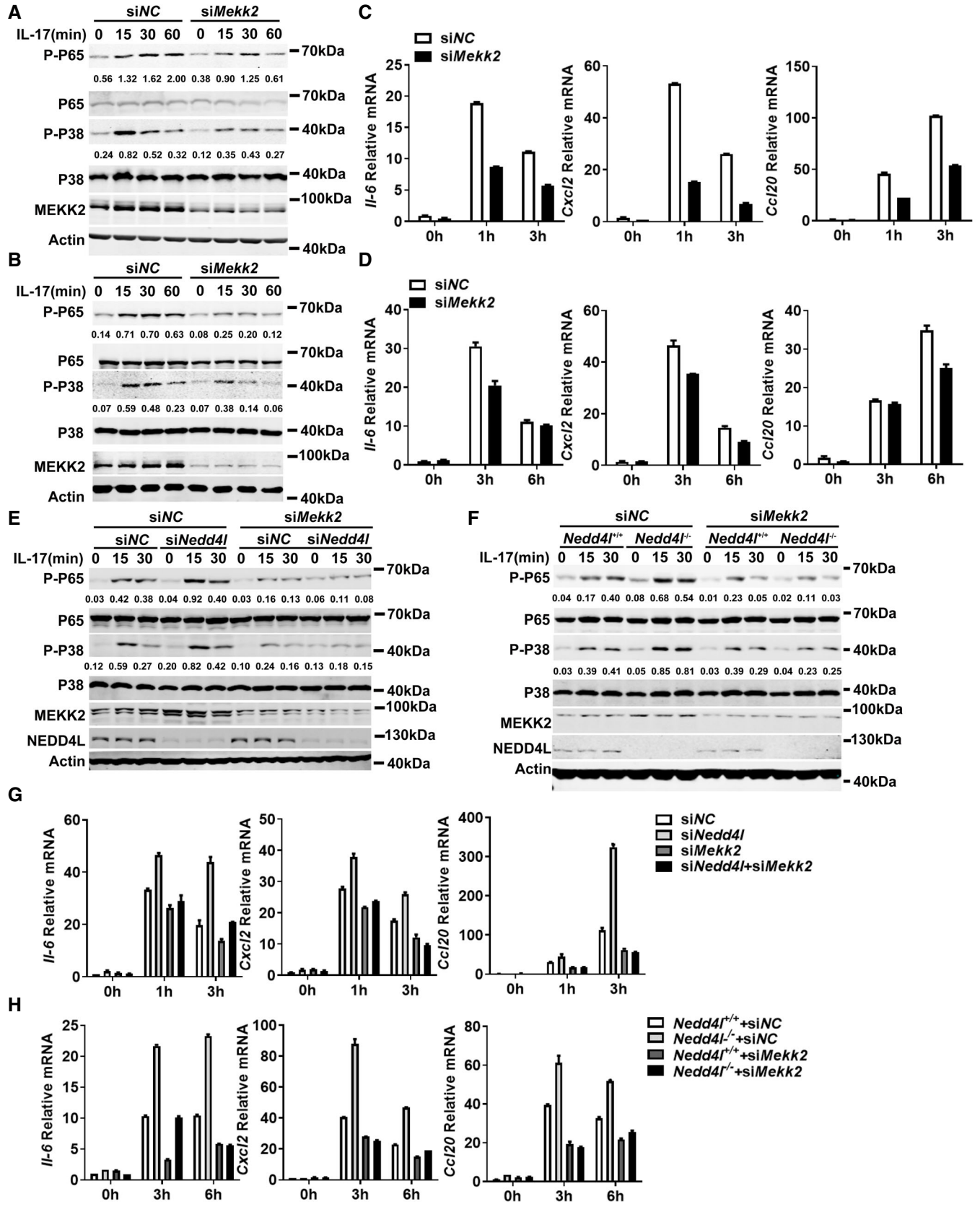

Figure 5.

cells. However, in the presence of *Mekk2* siRNA, *Nedd4l* siRNA could not enhance IL-17-induced p38 and NF-κB activation (Fig 5E). Similarly, *Mekk2* siRNA eliminated the enhancement of IL-17-induced p38 and NF-κB activation by *Nedd4l* deficiency in MEFs (Fig 5F). *Mekk2* knockdown nearly completely reversed the increase in IL-17-induced *Il-6*, *Cxcl2*, and *Ccl20* mRNA expression by *Nedd4l* knockdown in HeLa cells or *Nedd4l* deficiency in MEFs (Fig 5G and H). It has been identified that Smurf1, another HECT family E3, promotes MEKK2 ubiquitination and degradation in macrophages under the TLR9 activation (Wen *et al*, 2015). However, no combined effects were observed in *Smurf1* and *Nedd4l* combined silenced HeLa cells (Fig EV4C and D). Syk is known to be a target for NEDD4L in mast cells (Yip *et al*, 2016). Syk acts as an upstream signaling molecule in IL-17-induced Act1-TRAF6 interaction in keratinocytes, and inhibition of Syk can attenuate CCL20 production (Wu *et al*, 2015). We, therefore, checked the potential influence of Syk on NEDD4L-mediated IL-17 activation by treating HeLa cells with a Syk-specific inhibitor, BAY 61–3,606. As shown in Fig EV4E, specific inhibition of Syk attenuated IL-17-induced *Il-6*, *Cxcl2*, and *Ccl20* mRNA expression, but could not eliminate the enhancement of IL-17-induced *Il-6*, *Cxcl2*, and *Ccl20* mRNA expression by *Nedd4l* silencing in HeLa cells. These results demonstrate that NEDD4L negatively regulates IL-17R signaling via MEKK2.

MEKK2 Ser520 phosphorylation is required for IL-17R signaling and its degradation

MEKK2 Ser520 was reported to be phosphorylated following LPS stimulation and important for MEKK2 activation (Zhang *et al*, 2006). We prepared a phosphorylated MEKK2 Ser520-specific antibody to detect MEKK2 phosphorylation in IL-17-treated HeLa cells. As shown in Fig 6A, IL-17 stimulation induced remarkable MEKK2 Ser520 phosphorylation. The antibody against MEKK Ser520 was validated by western blotting analysis of wild-type MEKK2 and its Ser520 mutants, including MEKK2 Ser520 residue mutating into continuously activated forms asparagine (S520D) and glutamic acid (S520E), or inactivated form alanine (S520A; Figs EV4F and EV4G). As the Ser520 phosphorylation in MEKK2 is regulated by IL-17R signaling, we, therefore, tested if this phosphorylation is crucial for IL-17-induced proinflammatory cytokine and chemokine expression by mutating MEKK2 Ser520 residue into alanine (S520A). As shown in Fig 6B, MEKK2 S520A significantly inhibited the IL-17-induced proinflammatory cytokine and chemokine expression in HeLa cells, as well as the phosphorylation of p38 and NF-κB p65 (Fig 6C). Reconstitution of exogenous wild-type MEKK2, but not MEKK2-S520A, can restore the phosphorylation of p38 and NF-κB p65 in *Mekk2*-silenced HeLa cells compared to the control group (Fig EV4H).

We next explored how MEKK2 was activated in IL-17R signaling. IL-17 activates MAPK and NF-κB through the Act1-TRAF6-TAK1 cascade. We examined whether MEKK2 interacts with these molecules by immunoprecipitation. TAK1 was found to associate with MEKK2 following IL-17 stimulation (Fig 6D). We constructed plasmids expressing truncated MEKK2 N351 (a.a.1–351) and MEKK2 C352 (a.a.352–619; Fig EV4I). As shown in Fig EV4J, wild-type MEKK2, mutant MEKK2 S520A, and MEKK2 C352 could be co-immunoprecipitated with TAK1. In contrast, MEKK2 N351 could not be co-immunoprecipitated with TAK1, demonstrating that TAK1 interacted with the C-terminal kinase domain of MEKK2. We used *Tak1*-specific siRNA to inhibit endogenous TAK1 expression (Fig 6E). *Tak1* knockdown nearly completely blocked IL-17-induced MEKK2 phosphorylation (Fig 6E). These results suggest that MEKK2 interacts with TAK1 and is activated by TAK1 in IL-17R signaling.

We further investigated the effects of MEKK2 Ser520 phosphorylation on NEDD4L-mediated MEKK2 degradation. As shown in Fig 6F, NEDD4L was co-immunoprecipitated with MEKK2 (S520A) as efficiently as with wild-type MEKK2, indicating that MEKK2 Ser520 phosphorylation was not required for the association between NEDD4L and MEKK2. However, NEDD4L failed to promote MEKK2 (S520A) ubiquitination and degradation (Fig 6G and H), demonstrating that MEKK2 Ser520 phosphorylation is indispensable for NEDD4L-mediated MEKK2 ubiquitination. Taken together, IL-17 induces MEKK2 S520 phosphorylation, which is required for downstream p38 and NF-κB pathway activation. NEDD4L negatively regulates IL-17R signaling via mediating Ser520-phosphorylated MEKK2 degradation.

Figure 6. IL-17-induced MEKK2 Ser520 phosphorylation via TAK1 and promotes NEDD4L-mediated MEKK2 ubiquitination.

A Immunoblot analysis of Ser520 phosphorylation of MEKK2 immunoprecipitated from HeLa cells stimulated with IL-17 (50 ng/ml) for the indicated time, and then incubated with or without calf intestinal alkaline phosphatase time (CIAP) for 30 min.

B Real-time PCR analysis of *Il-6*, *Cxcl2*, and *Ccl20* mRNA expression in HeLa cells transfected with HA-tagged MEKK2 S520A or control vector, and stimulated with IL-17 (50 ng/ml) for the indicated time (n = 3 technical replicates).

C Immunoblot analysis of phosphorylated p38, phosphorylated NF-κB p65 (P-P65), HA, and actin in HeLa cells treated as in (B). Numbers between two blots indicate the densitometry of phosphorylated proteins relative to that of total proteins, respectively.

D Immunoblot analysis of MEKK2 and TAK1 co-immunoprecipitated with anti-TAK1 antibody from lysates of HeLa cells treated with 50 ng/ml IL-17 for the indicated time.

E Immunoblot analysis of Ser520 phosphorylation of MEKK2 immunoprecipitated from HeLa cells transfected with Tak1-specific (si*Tak1*) or control RNA (si*NC*), and then stimulated with IL-17 (50 ng/ml) for the indicated time.

F Immunoblot analysis of Myc-tagged NEDD4L co-immunoprecipitated with anti-HA antibody from lysates of HEK293T cells co-transfected with plasmids expressing Myc-tagged NEDD4L and HA-tagged wild-type MEKK2 or mutant MEKK2 (S520A).

G Immunoblot analysis of total ubiquitination of HA-tagged MEKK2 and HA-tagged MEKK2 (S520A) following precipitation of MEKK2 with anti-HA antibody from lysates of HEK293T cells co-transfected with plasmids expressing HA-tagged MEKK2 or HA-tagged MEKK2 (S520A) together with Myc-tagged NEDD4L and Flag-tagged Ub.

H Immunoblot analysis of HA-tagged MEKK2, HA-tagged MEKK2 (S520A), Myc-tagged NEDD4L, and actin in HEK293T cells transfected with the indicated plasmids with anti-HA, anti-Myc, or anti-actin antibody.

Data information: Data are shown as the mean ± S.E.M. of technical replicates. All experiments were performed two times, and representative data are shown.
Source data are available online for this figure.

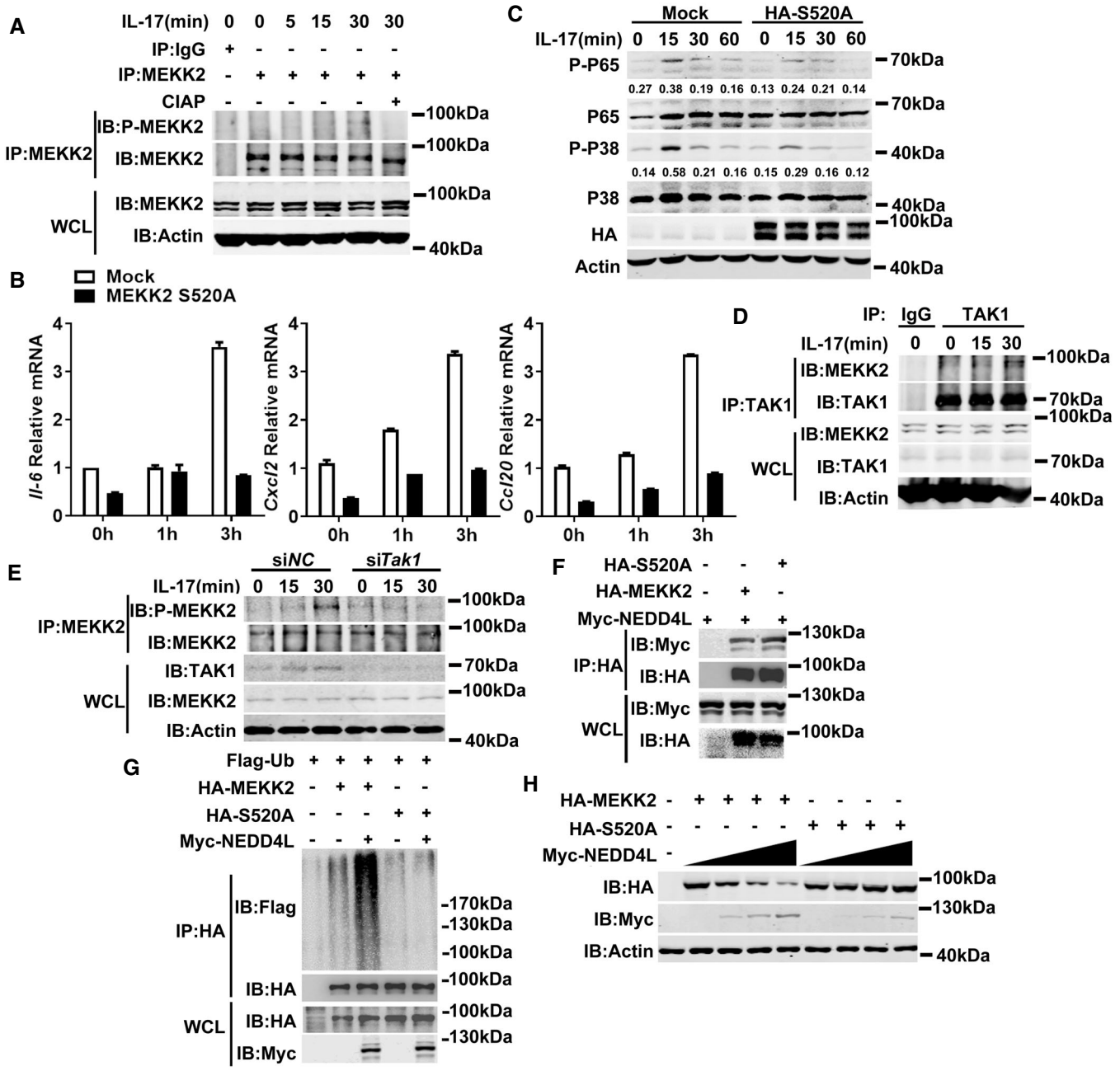

Figure 6.

Nedd4l deficiency promotes the pathogenesis of EAE via IL-17R-mediated inflammation in mice

It has been reported that IL-17R signaling in astrocytes plays a crucial role in mouse EAE, a well-known mouse multiple sclerosis (MS) model (Kang *et al*, 2010). We then investigated the effect of NEDD4L heterozygous deficiency on the MOG_{35-55}-induced EAE model by subcutaneous immunization of $Nedd4l^{+/+}$ or $Nedd4l^{+/-}$ mice with MOG_{35-55} and then intravenously injecting them with pertussis toxin (PTX). As shown in Fig EV5A, $Nedd4l^{+/-}$ mice suffered from more severe EAE disease symptoms compared to $Nedd4l^{+/+}$ mice and had higher EAE clinical scores than their counterparts. Moreover, $Nedd4l^{+/-}$ mice displayed more inflammatory cell infiltration and more serious demyelination compared to their counterparts (Fig EV5B), as demonstrated by hematoxylin–eosin (H&E) and Luxol fast blue (LFB) staining, respectively. Consistent with these results, flow cytometry analysis of mouse CNS tissues (brains and spinal cords) demonstrated that CNS-infiltrating $CD11b^{high}Gr1^{+}$ neutrophils were significantly increased in $Nedd4l^{+/-}$ mice compared to $Nedd4l^{+/+}$ mice (Fig EV5C–F). We subsequently examined the expression levels of several proinflammatory cytokines and chemokines in the CNS tissues of $Nedd4l^{+/+}$ and $Nedd4l^{+/-}$ EAE mice. As shown in Fig EV5G, the gene expression levels of *Il-6*, *Cxcl2*, and *Ccl20* were significantly increased in $Nedd4l^{+/-}$ EAE

mice. These data demonstrate that *Nedd4l* deficiency promotes the pathogenesis of EAE.

We next investigated whether the increased EAE pathogenesis in $Nedd4l^{+/-}$ mice is dependent on IL-17R-mediated signaling and inflammation. An anti-IL-17-specific blocking antibody was continually *i.p.* injected into $Nedd4l^{+/+}$ and $Nedd4l^{+/-}$ mice during the induction of EAE. As shown in Fig 7A and B, the injection of anti-IL-17 antibody resulted in significant inhibition of EAE disease symptoms, including clinical score, inflammation, and demyelination, in $Nedd4l^{+/+}$ and $Nedd4l^{+/-}$ mice compared to the anti-isotype control antibody-injected group. The $Nedd4l^{+/-}$ mice exhibited much more severe EAE disease symptoms compared to $Nedd4l^{+/+}$, which was obliterated after the injection of IL-17-blocking antibody (Fig 7A and B). Flow cytometry and real-time PCR analysis of mouse CNS tissues demonstrated that CNS-infiltrating $CD11b^{high}Gr1^{+}$ neutrophils and IL-17-induced genes, such as *Il-6*, *Cxcl2*, and *Ccl20*, were significantly reduced in IL-17-blocking antibody-treated $Nedd4l^{+/-}$ mice compared to mice treated with anti-isotype control antibody, which was obliterated after the injection of IL-17-blocking antibody (Fig 7C–E). However, continual *i.p.* injection of a Syk-specific inhibitor during the induction of EAE, BAY 61-3606, could not eliminate the EAE phenotype difference between $Nedd4l^{+/+}$ and $Nedd4l^{+/-}$ mice, suggesting that *Nedd4l* deficiency promotes the pathogenesis of EAE independent of Syk-mediated signaling (Fig 7F and G). Collectively, these data suggest that NEDD4L regulates EAE pathogenesis via IL-17R-mediated MEKK2-dependent signaling.

Discussion

In the present study, we show that endogenous NEDD4L inhibits IL-17, IL-1α, and TNF-α-induced proinflammatory cytokine and chemokine production. NEDD4L promotes MEKK2 ubiquitination and inhibits the protein stability of MEKK2, which is required for IL-17-, TNF-α-, and IL-1α-induced signaling.

NEDD4L is a highly conserved HECT-type E3 ligase. It has been reported to be involved with multi-physiological functions in mice by targeting the degradation of many important signal transduction-associated proteins (Manning & Kumar, 2018). Here, we identified NEDD4L as a negative regulator of IL-17-mediated inflammation by showing that *Nedd4l* knockdown and *Nedd4l* deficiency increased IL-17-induced proinflammatory cytokine and chemokine production. Even heterozygous deficiency of *Nedd4l* significantly increased IL-17-induced proinflammatory cytokine and chemokine production *in vitro* and *in vivo*, emphasizing the importance of NEDD4L in the negative regulation of IL-17R signaling.

IL-17 functions mainly by activating NF-κB and MAPK pathways to induce proinflammatory cytokine and chemokine production. Although NF-κB and MAPK activations have been demonstrated to be signal events downstream of adaptor protein Act1 and TRAF family members in IL-17R signaling, the detailed mechanisms by which NF-κB and MAPK are activated in IL-17R signaling remain largely unknown. MAP3K family members TAK1 and Tpl2 have been involved in IL-17-induced NF-κB and MAPK activation (Xiao *et al*, 2014). MEKK2 is involved in signal transduction of TCR, BMP, TGF-β, FGF-2, IL-1α, TNF-α, and TLR9 agonist CpG (Hammaker *et al*, 2004; Kesavan *et al*, 2004; Yamashita *et al*, 2005; Chang *et al*, 2011; Wen *et al*, 2015; Wu *et al*, 2021). Our results demonstrate that MEKK2 is required for IL-17-induced p38 and NF-κB activation in HeLa cells and MEFs. NEDD4L constitutively and directly binds MEKK2 and inhibits MEKK2 expression by promoting K27-linked poly-ubiquitination of MEKK2. *Mekk2* knockdown completely reverses *Nedd4l* deficiency mediated increase in IL-17-induced p38 and NF-κB activation, and also completely reverses the increase in IL-17-induced cytokine and chemokine production, clearly demonstrating that NEDD4L negatively regulates IL-17R signaling by inhibiting MEKK2 expression. In this study, we also show that NEDD4L inhibits TNF-α- and IL-1α-induced signaling, which has been reported to require MEKK2 to activate JNK and NF-κB pathways (Zhao & Lee, 1999; Hammaker *et al*, 2004).

IL-17, as well as TNF-α, are important for host immune defense against certain pathogens. However, excessive IL-17 activities have a high potential to induce damage to inflamed tissues. Thus, it is not surprising that multiple mechanisms restrict IL-17R signaling to avoid pathogenic conditions. Several IL-17R signaling negative regulators have been reported, including TRAF3, USP25, A20, $SCF^{\beta\text{-}TrCP}$, and GSK-3β (Zhong *et al*, 2012; Garg *et al*, 2013) (Shen *et al*, 2009; Zhu *et al*, 2010; Shi *et al*, 2011). We show here that NEDD4L negatively regulates IL-17R signaling via mediating MEKK2 ubiquitination. Upon IL-17 stimulation, MEKK2 is phosphorylated at Ser520, which is crucial not only for the activation of p38 and NF-κB

Figure 7. *Nedd4l* deficiency inhibits $MOG_{35\text{-}55}$-induced EAE via IL-17-dependent manner.

A *Nedd4l*$^{+/+}$ and *Nedd4l*$^{+/-}$ mice (*Nedd4l*$^{+/+}$ $n = 5$ biological replicates and *Nedd4l*$^{+/-}$ $n = 4$ biological replicates) were treated with intraperitoneal (*i.p.*) injection of an anti-IL-17A antibody (100 μg per mouse each time) or appropriate isotype control anti-IgG antibody on days 7, 9, 11, and 13 after the second $MOG_{35\text{-}55}$ immunization. Mean clinical scores were calculated every other day according to the standards described in the Materials and Methods.

B Histology of the spinal cord was analyzed by H&E (up panel) or LFB (down panel) staining on day 14 after the second $MOG_{35\text{-}55}$ immunization. Scale bars, 500 μm.

C, D Summary graph of the percentages of immune cells in the CNS. CNS-infiltrating cells isolated from mice treated as in (A) were stained with the appropriate antibodies (*Nedd4l*$^{+/+}$ $n = 5$ biological replicates and *Nedd4l*$^{+/-}$ $n = 4$ biological replicates).

E *Il-6*, *Cxcl2*, and *Ccl20* mRNA in the CNS tissues from mice treated as in (A) (including brain and spinal cords) were measured by real-time PCR on day 14 after the second $MOG_{35\text{-}55}$ immunization (*Nedd4l*$^{+/+}$ $n = 5$ biological replicates and *Nedd4l*$^{+/-}$ $n = 4$ biological replicates).

F *Nedd4l*$^{+/+}$ and *Nedd4l*$^{+/-}$ mice (*Nedd4l*$^{+/+}$ $n = 5$ biological replicates and *Nedd4l*$^{+/-}$ $n = 7$ biological replicates) were treated with intraperitoneal (*i.p.*) injection of Syk-specific inhibitor BAY 61–3,606 (5 mg/kg each time) on days 7, 9, 11, and 13 after the second $MOG_{35\text{-}55}$ immunization. Mean clinical scores were assessed as in (A).

G Histology of the spinal cord was analyzed by H&E (left panel) or LFB (right panel) staining on day 14 after the second $MOG_{35\text{-}55}$ immunization. Scale, 500 μm.

Data information: Data are shown as the mean ± S.E.M. of biological replicates. All experiments were performed two times, and representative data are shown. Significant differences were tested using a two-tailed Mann–Whitney *U* test (A, F) or a two-tailed Student's *t*-test (C, D, E). $^{**}P < 0.01$ and $^{***}P < 0.001$. NS, no significance.

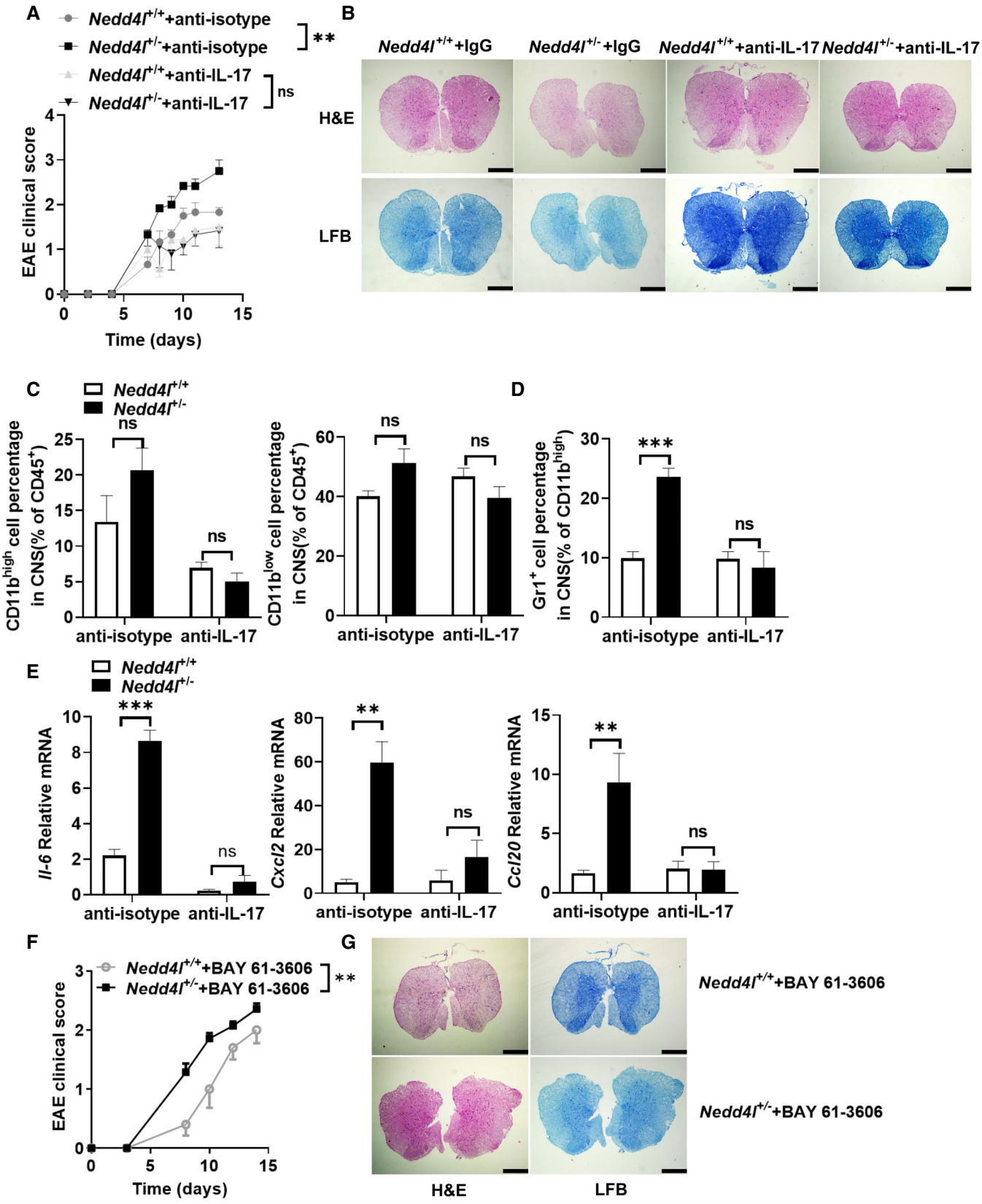
A
Nedd4l+/+ +anti-isotype
Nedd4l+/- +anti-isotype
Nedd4l+/+ +anti-IL-17
Nedd4l+/- +anti-IL-17
**
ns
EAE clinical score
Time (days)
B
Nedd4l+/+ +IgG
Nedd4l+/- +IgG
Nedd4l+/+ +anti-IL-17
Nedd4l+/- +anti-IL-17
H&E
LFB
C
Nedd4l+/+
Nedd4l+/-
CD11bhigh cell percentage in CNS(% of CD45+)
CD11blow cell percentage in CNS(% of CD45+)
anti-isotype
anti-IL-17
D
Gr1+ cell percentage in CNS(% of CD11bhigh)
***
E
Il-6 Relative mRNA
Cxcl2 Relative mRNA
Ccl20 Relative mRNA
F
Nedd4l+/+ +BAY 61-3606
Nedd4l+/- +BAY 61-3606
G
Nedd4l+/+ +BAY 61-3606
Nedd4l+/- +BAY 61-3606
H&E
LFB

Figure 7.

pathways but also for NEDD4L-mediated MEKK2 degradation that negatively regulates IL-17R-induced inflammation.

Excessive IL-17-, IL-1α-, and TNF-α-triggered signaling have been linked to the development of many inflammatory responses or autoimmune diseases. Our data show that *Nedd4l* deficiency in mice significantly promotes IL-17-induced pneumonia and peritonitis, and also MOG_{35-55}-induced EAE in IL-17R-signaling dependent manner. NEDD4L has also been identified to regulate phosphorylated-Syk K48-linked ubiquitination in mast cells (Yip *et al*, 2016), and Syk acts as an upstream signaling molecule in IL-17-induced Act1-TRAF6 interaction in keratinocytes (Wu *et al*, 2015), suggesting that NEDD4L may regulate IL-17R signaling dependent on Syk. However, inhibition of Syk activation in HeLa cells and during induction of the MOG_{35-55}-induced EAE model did not eliminate the phenotype difference *in vitro* and *in vivo*, which means NEDD4L regulates IL-17R-mediated inflammation and EAE is not dependent on Syk in our experimental system. Taken together, these data confirm that NEDD4L plays a crucial role in IL-17R-mediated inflammation and EAE.

Taken together, the present study identifies MEKK2 as a mediator of IL-17R signaling, and NEDD4L as a common negative regulator of IL-17-, TNF-α-, and IL-1α-induced signaling by inhibiting MEKK2 expression, providing novel insights into the mechanism of IL-17-, TNF-α, and IL-1α-induced signaling. IL-17 stimulation induces the MEKK2 phosphorylation and degradation, which are required for the induction of proinflammatory cytokine and chemokine. Thus, based on our findings, NEDD4L serves as a functional protein in inflammation and autoimmune diseases. NEDD4L could be a target for the treatment of IL-17R-related inflammation and autoimmune disorders.

Materials and Methods

Mice

Nedd4l-deficient homozygous ($Nedd4l^{-/-}$) and control BALB/cByJ ($Nedd4l^{+/+}$) mice were purchased from JAX® Mice, America. In this study, *Nedd4l*-deficient homozygous $Nedd4l^{+/-}$ mice were used *in vivo* diseases research for $Nedd4l^{-/-}$ mice show kidney defects and some other problems (Manning & Kumar, 2018). Off-springs of the mice at the age of 6–8 weeks were employed in experiments. All animal experiments were carried out under the National Institute of Health Guide for the Care and Use of Laboratory Animals, with the approval of the Scientific Investigation Board of Laboratory Animal Center of Zhejiang University.

Reagents

Antibodies for phospho-ERK1/2 (#4370S), phospho-JNK (#9251S), phospho-p38 (#4511S), phospho-p65 (NF-κB) (#3033 s), ERK1/2 (#4696), JNK (#9251 s), p38 (#8690), NF-κB p65 (#8242), and NEDD4L (#4013) were from Cell Signaling Technology (Cell Signaling Technology, Beverly, MA). Antibodies for TRAF2 (#5525–1), MEKK3 (#1673–1), and MEKK5 (#1772–1) were from Epitomics (Epitomics, Burlingame, CA). Antibodies for TAK1 (SC-7967), MEKK2 (SC-1088), TRAF3 (SC-949), and TRAF6 (SC-7221) were obtained from Santa Cruz Biotechnology (Santa Cruz Biotechnology, Santa Cruz, CA). Phospho-MEKK2 Ser520-specific antibody was prepared in Abmart (Shanghai, China). Human or mouse IL-17A/F (human IL-17, #200–17; Murine IL-17A, #210–17; human IL-17F, #200–25; and murine IL-17F, #210-17F) were purchased from PeproTech (PeproTech, Rocky Hill, NJ). E1, UBCH5b, and ubiquitin recombinant proteins were gifts from Prof. Zongping Xia (Zhejiang University).

Plasmids

To construct a plasmid-expressing Myc-tagged NEDD4L, cDNA-encoding NEDD4L was amplified by PCR using mRNA of mouse peritoneal macrophage as a template, and cloned in the pCMV-Entry plasmid. Flag-tag in the plasmid was deleted by PCR and the plasmid could express Myc-tagged NEDD4L. MEKK2 cDNA was amplified by PCR using mRNA of HeLa cells as a template and cloned in pCMV-HA or pcDNA3.1 plasmid. The vectors for NEDD4L and MEKK2 mutants were subsequently generated by PCR amplification.

IL-17-induced peritoneal inflammatory responses

Male age-matched $Nedd4l^{+/+}$ and $Nedd4l^{+/-}$ littermates were treated by intraperitoneal injection of IL-17 (0.5 μg per mouse) or PBS. Twenty-four hours later, intraperitoneal leukocytes were removed by washing the peritoneal cavity with 5 ml PBS. And then 5 ml of 0.25% trypsin was injected into the peritoneal cavity. Ten minutes later, the trypsin solution was collected, and then 5 ml DMEM containing 10% FBS was used to wash the peritoneal cavity and residual mesothelial cells were collected. The expression of chemokines in the cells was measured by real-time PCR analysis (Zhong *et al*, 2012).

IL-17-induced pulmonary inflammation

Male age-matched $Nedd4l^{+/+}$ and $Nedd4l^{+/-}$ littermates were treated by intratracheal injection of IL-17 (2 μg per mouse, 30 μl) or PBS (30 μl). Eight hours later, BLAF fluid was collected in 1.2 ml ice-cold PBS through the trachea and centrifuged. Chemokines and cytokines in the supernatants were measured using ELISA assays. Cells in the precipitates were resuspended using 0.1 ml staining buffer and counted as lung-infiltrating cells. The cells were also analyzed using flow cytometry after staining with anti-Gr-1 and anti-CD11b antibodies. The total RNA of the lung tissues was isolated with 1 ml ice-cold TriZol for real-time PCR analysis. Lung tissues were dissected, fixed in 4% paraformaldehyde, embedded in paraffin, sectioned, and then stained with hematoxylin and eosin (Bulek *et al*, 2011).

Pull-down assay

GST-tagged MEKK2 (M0324) and Myc-tagged NEDD4L recombinant proteins were purchased from Sigma and Origene (Origene, Rockville, MD), respectively. GST-MEKK2 (0.1 μg) bound to glutathione-agarose beads were mixed with 0.05 μg Myc-tagged NEDD4L and incubated at 4°C for 4 h with gentle rotation. The beads were washed three times with cell lysis buffer. Then, bound proteins were extracted with loading buffer and analyzed by immunoblot (Xia *et al*, 2009).

Ubiquitination assay

For *in vivo* ubiquitination assay, HEK293T cells were transfected with pCDNA3.1-HA ubiquitin along with other vectors as indicated and cultured for 36 h. After being treated with MG-132 for 6 h, the cells were lysed in 1% SDS and then heated for 5 min. After centrifuging, the supernatants were 10-fold diluted with lysis buffer, followed by immunoprecipitation with the appropriate antibodies. Immunoprecipitants were analyzed by immunoblot with anti-ubiquitin or antibody specific for K63-linked ubiquitin/K48-linked ubiquitin. The *in vitro* MEKK2 ubiquitination assay was carried out in a reaction mixture containing 0.2 μM E1, 0.1 μM UBCH5b, 0.4 μM Myc-tagged NEDD4L, and 12.5 μM ubiquitin in buffer B at 30°C for 60 min before termination with SDS-sample buffer (Xia *et al*, 2009).

Induction and assessment of EAE

Acute EAE was induced and assessed as previously described (Kang *et al*, 2010). Briefly, acute EAE was induced by subcutaneous immunization with 300 μg of the MOG_{35-55} peptide (Met-Glu-Val-Gly-Trp-Tyr-Arg-Ser-Pro-Phe-Ser-Arg-Val-Val-His-Leu-Tyr-Arg-Asn-Gly-Lys, Sangon Biotech Co.) in CFA containing 5 mg/ml heat-killed H37Ra strain of *Mycobacterium tuberculosis* (Chondrex, Inc) in the back region and both sides of the vertebrae. And the immunized mice were i.v. injected with pertussis toxin (List Biological Laboratories, Inc.) at a dose of 250 ng per mouse in PBS on the day of immunization and once more 48 h after the first injection. The clinical score was performed in a double-blinded manner. Mice were examined every 2–3 days for disease symptoms and were double-blinded and scored for disease severity using the EAE scoring rulers: 0, no clinical signs; 1, limp tail; 2, paraparesis (weakness and incomplete paralysis of one or two hind limbs); 3, paraplegia (complete paralysis of two hind limbs); 4, paraplegia with fore limb weakness or paralysis; and 5, moribund state or death.

Isolation and analysis of CNS inflammatory cells

Central nervous system tissues, including spinal cords and brains, were homogenized in ice-cold tissue grinders, filtered through a 70 μm cell strainer (Falcon), and the cells were collected by centrifugation at 160 *g* for 5 min at 4°C. Cells were re-suspended in 10 ml of 35% Percoll (GE) and centrifuged onto a 5 ml 70% Percoll cushion in 15-ml tubes at 280 *g* for 25 min with a low accelerating or breaking speed. Cells at the 35–70% interface were collected and subjected to flow cytometry. Fluorescence-conjugated monoclonal antibodies to FVD, CD45, CD4, CD8, CD11b, F4/80, and Gr-1 were stained together for the surface marker analysis.

Histological analysis

Paraffin-embedded sections (4 mm thick) were subjected to either hematoxylin and eosin (H&E) or Luxol fast blue (LFB) to evaluate inflammation and demyelination, respectively. H&E and LFB were performed by the Histomorphology Platform, Zhejiang University, with the standard protocol performed according to the manufacturer's instructions.

Real-time quantitative PCR and ELISA

Total RNA was isolated using TRIzol (TAKARA, Ostushiga, JAPAN) and cDNA was synthesized with a reverse-transcription kit (TAKARA, Ostushiga, JAPAN). The expression of genes was detected by a LightCycler 480 system with SYBR Premix Ex Tap (TAKARA, Ostushiga, JAPAN). The data were calculated by a standard curve method and normalized to the expression of the gene-encoding *gapdh* (human) or *β-actin* (mouse). The specific primers for individual genes are in Appendix Table S1. The concentration of cytokines and chemokines in the cell culture medium was detected by ELISA assay (ebioscience, MN, USA and R&D, CA, USA).

Statistical analysis

The statistical analysis was performed using a two-tailed Mann–Whitney *U* test or a two-tailed Student's *t*-test. Differences were considered significant at a P value of < 0.05.

Data availability

No primary datasets have been generated and deposited.

Expanded View for this article is available online.

Acknowledgements

This work is supported by grants from the National Key Basic Research Program of China (2014CB542101 and 2013CB531606), National Natural Science Foundation of China (82071774, 31770932, 31970899, 81373153, and 81571550), Natural Science Foundation of Zhejiang Province (LZ22H100001, LR13C080001, LY19H160048, LY20H050006, and LY15H160006), Shanghai Key Laboratory of Cell Engineering (14DZ2272300), and Shanghai Leading Academic Discipline Project (B905).

Author contributions

Ning Wang: Data curation; software; formal analysis; validation; methodology. **Yu Jiang:** Resources; funding acquisition; validation. **Huazhang An:** Conceptualization; resources; funding acquisition; validation; methodology; writing – original draft; writing – review and editing. **Haofei Wang:** Validation; methodology. **Hui Li:** Conceptualization; resources; data curation; software; formal analysis; funding acquisition; validation; investigation; methodology; writing – original draft; writing – review and editing. **Wenlong Lin:** Conceptualization; formal analysis; funding acquisition; investigation; writing – original draft; project administration; writing – review and editing. **Wangqian Ma:** Resources; funding acquisition. **Zengfeng Xin:** Resources; funding acquisition. **Hao Pan:** Resources; funding acquisition. **Xiaojian Wang:** Conceptualization; resources; formal analysis; supervision; writing – original draft; project administration; writing – review and editing. **Ting Zhang:** Resources; funding acquisition; project administration.

In addition to the CRediT author contributions listed above, the contributions in detail are:

HL, WL, NW, and HW performed experiments. HL and WL performed the statistical analysis. YJ, ZX, HP, WM, and TZ provided some reagents. HA, XW, WL, and HL designed the study. HL, XW, WL, and HA drafted the manuscript.

Disclosure and competing interests statement

The authors declare that they have no conflict of interest.

References

Abriel H, Loffing J, Rebhun JF, Pratt JH, Schild L, Horisberger JD, Rotin D, Staub O (1999) Defective regulation of the epithelial Na+ channel by Nedd4 in Liddle's syndrome. *J Clin Invest* 103: 667 – 673

Blonska M, You Y, Geleziunas R, Lin X (2004) Restoration of NF-kappaB activation by tumor necrosis factor alpha receptor complex-targeted MEKK3 in receptor-interacting protein-deficient cells. *Mol Cell Biol* 24: 10757 – 10765

Boraschi D, Italiani P, Weil S, Martin MU (2018) The family of the interleukin-1 receptors. *Immunol Rev* 281: 197 – 232

Bulek K, Liu C, Swaidani S, Wang L, Page RC, Gulen MF, Herjan T, Abbadi A, Qian W, Sun D *et al* (2011) The inducible kinase IKKi is required for IL-17-dependent signaling associated with neutrophilia and pulmonary inflammation. *Nat Immunol* 12: 844 – 852

Catrysse L, Vereecke L, Beyaert R, van Loo G (2014) A20 in inflammation and autoimmunity. *Trends Immunol* 35: 22 – 31

Chang X, Liu F, Wang X, Lin A, Zhao H, Su B (2011) The kinases MEKK2 and MEKK3 regulate transforming growth factor-beta-mediated helper T cell differentiation. *Immunity* 34: 201 – 212

Charbonnier-Beaupel F, Malerbi M, Alcacer C, Tahiri K, Carpentier W, Wang C, During M, Xu D, Worley PF, Girault JA *et al* (2015) Gene expression analyses identify Narp contribution in the development of L-DOPA-induced dyskinesia. *J Neurosci* 35: 96 – 111

Chayama K, Papst PJ, Garrington TP, Pratt JC, Ishizuka T, Webb S, Ganiatsas S, Zon LI, Sun W, Johnson GL *et al* (2001) Role of MEKK2-MEK5 in the regulation of TNF-alpha gene expression and MEKK2-MKK7 in the activation of c-Jun N-terminal kinase in mast cells. *Proc Natl Acad Sci U S A* 98: 4599 – 4604

Coussens LM, Werb Z (2002) Inflammation and cancer. *Nature* 420: 860 – 867

Gaffen SL (2009) Structure and signalling in the IL-17 receptor family. *Nat Rev Immunol* 9: 556 – 567

Gao S, Alarcon C, Sapkota G, Rahman S, Chen PY, Goerner N, Macias MJ, Erdjument-Bromage H, Tempst P, Massague J (2009) Ubiquitin ligase Nedd4L targets activated Smad2/3 to limit TGF-beta signaling. *Mol Cell* 36: 457 – 468

Gao P, Ma X, Yuan M, Yi Y, Liu G, Wen M, Jiang W, Ji R, Zhu L, Tang Z *et al* (2021) E3 ligase Nedd4l promotes antiviral innate immunity by catalyzing K29-linked cysteine ubiquitination of TRAF3. *Nat Commun* 12: 1194

Garg AV, Ahmed M, Vallejo AN, Ma A, Gaffen SL (2013) The deubiquitinase A20 mediates feedback inhibition of interleukin-17 receptor signaling. *Sci Signal* 6: ra44

Goulet CC, Volk KA, Adams CM, Prince LS, Stokes JB, Snyder PM (1998) Inhibition of the epithelial Na+ channel by interaction of Nedd4 with a PY motif deleted in Liddle's syndrome. *J Biol Chem* 273: 30012 – 30017

Hammaker DR, Boyle DL, Chabaud-Riou M, Firestein GS (2004) Regulation of c-Jun N-terminal kinase by MEKK-2 and mitogen-activated protein kinase kinase kinases in rheumatoid arthritis. *J Immunol* 172: 1612 – 1618

Hotamisligil GS (2017) Inflammation, metaflammation and immunometabolic disorders. *Nature* 542: 177 – 185

Iwakura Y, Ishigame H, Saijo S, Nakae S (2011) Functional specialization of interleukin-17 family members. *Immunity* 34: 149 – 162

Jewett KA, Christian CA, Bacos JT, Lee KY, Zhu J, Tsai NP (2016) Feedback modulation of neural network synchrony and seizure susceptibility by Mdm2-p53-Nedd4-2 signaling. *Mol Brain* 9: 32

Kalliolias GD, Ivashkiv LB (2016) TNF biology, pathogenic mechanisms and emerging therapeutic strategies. *Nat Rev Rheumatol* 12: 49 – 62

Kang Z, Altuntas CZ, Gulen MF, Liu C, Giltiay N, Qin H, Liu L, Qian W, Ransohoff RM, Bergmann C *et al* (2010) Astrocyte-restricted ablation of interleukin-17-induced Act1-mediated signaling ameliorates autoimmune encephalomyelitis. *Immunity* 32: 414 – 425

Kesavan K, Lobel-Rice K, Sun W, Lapadat R, Webb S, Johnson GL, Garrington TP (2004) MEKK2 regulates the coordinate activation of ERK5 and JNK in response to FGF-2 in fibroblasts. *J Cell Physiol* 199: 140 – 148

Liu CH, Chen Z, Chen K, Liao FT, Chung CE, Liu X, Lin YC, Keohavong P, Leikauf GD, Di YP (2020) Lipopolysaccharide-mediated chronic inflammation promotes tobacco carcinogen-induced lung cancer and determines the efficacy of immunotherapy. *Cancer Res* 81: 144 – 157

Liu H, Lin W, Liu Z, Song Y, Cheng H, An H, Wang X (2021) E3 ubiquitin ligase NEDD4L negatively regulates keratinocyte hyperplasia by promoting GP130 degradation. *EMBO Rep* 22: e52063

Lorenz S (2018) Structural mechanisms of HECT-type ubiquitin ligases. *Biol Chem* 399: 127 – 145

Malonis RJ, Fu W, Jelcic MJ, Thompson M, Canter BS, Tsikitis M, Esteva FJ, Sanchez I (2017) RNF11 sequestration of the E3 ligase SMURF2 on membranes antagonizes SMAD7 down-regulation of transforming growth factor beta signaling. *J Biol Chem* 292: 7435 – 7451

Manning JA, Kumar S (2018) Physiological functions of Nedd4-2: Lessons from knockout mouse models. *Trends Biochem Sci* 43: 635 – 647

Maspero E, Valentini E, Mari S, Cecatiello V, Soffientini P, Pasqualato S, Polo S (2013) Structure of a ubiquitin-loaded HECT ligase reveals the molecular basis for catalytic priming. *Nat Struct Mol Biol* 20: 696 – 701

Medzhitov R (2008) Origin and physiological roles of inflammation. *Nature* 454: 428 – 435

Qu F, Gao H, Zhu S, Shi P, Zhang Y, Liu Y, Jallal B, Yao Y, Shi Y, Qian Y (2012) TRAF6-dependent Act1 phosphorylation by the IkappaB kinase-related kinases suppresses interleukin-17-induced NF-kappaB activation. *Mol Cell Biol* 32: 3925 – 3937

Rostami A, Ciric B (2013) Role of Th17 cells in the pathogenesis of CNS inflammatory demyelination. *J Neurol Sci* 333: 76 – 87

Shen F, Li N, Gade P, Kalvakolanu DV, Weibley T, Doble B, Woodgett JR, Wood TD, Gaffen SL (2009) IL-17 receptor signaling inhibits C/EBPbeta by sequential phosphorylation of the regulatory 2 domain. *Sci Signal* 2: ra8

Shi P, Zhu S, Lin Y, Liu Y, Liu Y, Chen Z, Shi Y, Qian Y (2011) Persistent stimulation with interleukin-17 desensitizes cells through SCFbeta-TrCP-mediated degradation of Act1. *Sci Signal* 4: ra73

Sutton CE, Lalor SJ, Sweeney CM, Brereton CF, Lavelle EC, Mills KH (2009) Interleukin-1 and IL-23 induce innate IL-17 production from gammadelta T cells, amplifying Th17 responses and autoimmunity. *Immunity* 31: 331 – 341

Wang J, Peng Q, Lin Q, Childress C, Carey D, Yang W (2010) Calcium activates Nedd4 E3 ubiquitin ligases by releasing the C2 domain-mediated auto-inhibition. *J Biol Chem* 285: 12279 – 12288

Wen M, Ma X, Cheng H, Jiang W, Xu X, Zhang Y, Zhang Y, Guo Z, Yu Y, Xu H *et al* (2015) Stk38 protein kinase preferentially inhibits TLR9-activated inflammatory responses by promoting MEKK2 ubiquitination in macrophages. *Nat Commun* 6: 7167

Wolf Y, Shemer A, Polonsky M, Gross M, Mildner A, Yona S, David E, Kim KW, Goldmann T, Amit I *et al* (2017) Autonomous TNF is critical for in vivo monocyte survival in steady state and inflammation. *J Exp Med* 214: 905 – 917

Wu NL, Huang DY, Tsou HN, Lin YC, Lin WW (2015) Syk mediates IL-17-induced CCL20 expression by targeting Act1-dependent K63-linked ubiquitination of TRAF6. *J Invest Dermatol* 135: 490 – 498

Wu N, Sun H, Zhao X, Zhang Y, Tan J, Qi Y, Wang Q, Ng M, Liu Z, He L *et al* (2021) MAP3K2-regulated intestinal stromal cells define a distinct stem cell niche. *Nature* 592: 606 – 610

Xia ZP, Sun L, Chen X, Pineda G, Jiang X, Adhikari A, Zeng W, Chen ZJ (2009) Direct activation of protein kinases by unanchored polyubiquitin chains. *Nature* 461: 114 – 119

Xiao Y, Jin J, Chang M, Nakaya M, Hu H, Zou Q, Zhou X, Brittain GC, Cheng X, Sun SC (2014) TPL2 mediates autoimmune inflammation through activation of the TAK1 axis of IL-17 signaling. *J Exp Med* 211: 1689 – 1702

Yamashita M, Ying SX, Zhang GM, Li C, Cheng SY, Deng CX, Zhang YE (2005) Ubiquitin ligase Smurf1 controls osteoblast activity and bone homeostasis by targeting MEKK2 for degradation. *Cell* 121: 101 – 113

Yip KH, Kolesnikoff N, Hauschild N, Biggs L, Lopez AF, Galli SJ, Kumar S, Grimbaldeston MA (2016) The Nedd4-2/Ndfip1 axis is a negative regulator of IgE-mediated mast cell activation. *Nat Commun* 7: 13198

Zhang D, Facchinetti V, Wang X, Huang Q, Qin J, Su B (2006) Identification of MEKK2/3 serine phosphorylation site targeted by the toll-like receptor and stress pathways. *EMBO J* 25: 97 – 107

Zhao Q, Lee FS (1999) Mitogen-activated protein kinase/ERK kinase kinases 2 and 3 activate nuclear factor-kappaB through IkappaB kinase-alpha and IkappaB kinase-beta. *J Biol Chem* 274: 8355 – 8358

Zhong B, Liu X, Wang X, Chang SH, Liu X, Wang A, Reynolds JM, Dong C (2012) Negative regulation of IL-17-mediated signaling and inflammation by the ubiquitin-specific protease USP25. *Nat Immunol* 13: 1110 – 1117

Zhu S, Pan W, Shi P, Gao H, Zhao F, Song X, Liu Y, Zhao L, Li X, Shi Y *et al* (2010) Modulation of experimental autoimmune encephalomyelitis through TRAF3-mediated suppression of interleukin 17 receptor signaling. *J Exp Med* 207: 2647 – 2662